Magnetization Distribution in Ferromagnetic $MnPt_3$ by a Polarized-Neutron Investigation

B. ANTONINI, F. LUCARI, F. MENZINGER, AND A. PAOLETTI
Laboratorio Fisica Nucleare Applicata, Centro Studi Nucleari della Casaccia, Comitato Nazionale per l'Energia Nucleare, Rome, Italy
(Received 24 February 1969)

The magnetic electron distribution in $MnPt_3$ ferromagnetic alloy has been determined by the polarized neutron technique. The Mn form factor in the ferromagnetic state has been determined and agrees closely with the theoretical one calculated for the free atom. The magnetic moments are $(3.64\pm0.08)\mu_B$ for Mn atoms and $(0.26\pm0.03)\mu_B$ for Pt atoms. The magnetic electron distribution on Pt atoms is strongly aspherical. The tetragonal field splits the d levels into sublevels. The population of these sublevels has been estimated.

I. INTRODUCTION

THERE has been an increasing interest over the past few years in the magnetization distribution in alloys of the transition elements of the iron group with those of the palladium and platinum groups. Several neutron diffraction investigations have been performed at several laboratories. However, only a few measurements have been performed to establish the detailed unpaired electron density in the unit cell, so that extensive and systematic work is still needed in order to be able to draw general conclusions about this problem. Accordingly, we have undertaken a program of investigation of the magnetic electron distribution in ferromagnetic alloys of the $3d$-$4d$ and the $3d$-$5d$ types.[1–3]

Similar experiments, performed by the Brookhaven group, which studied FeRh [4] and $FePd_3$,[5] indicated quite definitely that the magnetic moments localized on the site of the non-$3d$ element have an electron distribution characteristic of that element. In most cases, it was possible to establish the electron population of the sublevels into which the d level is split by the crystalline field. The presence of negative magnetization was not ascertained in these alloys, although it was determined in the three ferromagnetic elements Fe,[6] Co,[7] and Ni.[8]

$MnPt_3$ alloy is ferromagnetic below 390°K and orders chemically, assuming the Cu_3Au superlattice, by annealing at temperatures below 950°C.[9] Therefore, it is suited for a detailed determination of the magnetic electron distribution by the polarized neutron technique.

In the course of a neutron diffraction investigation of the magnetic ordering in the ternary system Fe-Mn-Pt, Bacon and Mason[10] established the boundary of the ferromagnetic region around the $MnPt_3$ composition; the magnetic moment on Mn was found to be about 3.6 μ_B. The magnetic structures at other compositions in the Mn-Pt system were studied by Kren *et al.*[11–13] and by Andresen *et al.*[14] by means of neutron diffraction and were found to be antiferromagnetic. Magnetic moments of the order of 4 μ_B on Mn were found, while no magnetic moment was detected on the platinum sites. The ferromagnetic behavior of $MnPt_3$ appeared to be restricted to a relatively small range of composition; the substitution of Fe for Mn produced a change from ferromagnetism to antiferromagnetism.[10]

$MnPt_3$ powder samples have been studied in the past by Pickart and Nathans,[15] who assigned magnetic moments of (3.60 ± 0.09) and (0.17 ± 0.04) μ_B to manganese and platinum, respectively, under the hypothesis that the Pt form factor was negligible at reciprocal-lattice points other that the origin. However, it was later shown[2] that the Pt form factor is more expanded.

II. EXPERIMENTAL

A. Samples

Our samples were cut from a large single crystal.[16] All of them were then annealed 72 h at 850°C in order to establish long-range order of the Cu_3Au type. The long-range order parameter S was found to be 0.90 ± 0.02 by absolute measurements with x rays, and to be 0.92 ± 0.02 by neutron diffraction. Chemical analysis showed that the composition was stoichiometric within 0.2%. The samples used in the neutron diffraction ex-

[1] B. Antonini, G. P. Felcher, G. Mazzone, F. Menzinger, and A. Paoletti, in *Proceedings of the International Conference on Magnetism, Nottingham, 1964* (The Institute of Physics and the Physical Society, London, 1965), p. 288.
[2] F. Menzinger and A. Paoletti, Phys. Rev. **143**, 365 (1966).
[3] B. Antonini, F. Menzinger, and A. Paoletti, Phys. Letters **25A**, 372 (1967).
[4] G. Shirane, R. Nathans, and C. W. Chen, Phys. Rev. **134**, A1547 (1964).
[5] G. Shirane, R. Nathans, S. J. Pickart, and H. A. Alperin, in *Proceedings of the International Conference on Magnetism, Nottingham, 1964* (The Institute of Physics and the Physical Society, London, 1965), p. 223.
[6] C. G. Shull and H. A. Mook, Phys. Rev. Letters **16**, 184 (1966).
[7] R. M. Moon, Phys. Rev. **136**, 195 (1964).
[8] H. A. Mook, Phys. Rev. **148**, 495 (1966).
[9] M. Hansen, *Constitution of Binary Alloys* (McGraw-Hill Book Co., New York, 1958), p. 946.
[10] G. E. Bacon and E. W. Mason, Proc. Phys. Soc. (London) **88**, 929 (1966).
[11] E. Kren, M. Cselik, G. Kadar, and L. Pal, Phys. Letters **24**, 198 (1967).
[12] E. Kren, G. Kadar, L. Pal, J. Solyom, P. Szabo, and T. Tarnoczi, Phys. Rev. **171**, 574 (1968).
[13] E. Kren, G. Kadar, and P. Szabo, Phys. Letters **26A**, 556 (1968).
[14] A. F. Andresen, A. Kjekshuch, R. Moellerud, and W. B. Pearson, Phil. Mag. **11**, 1245 (1965).
[15] S. J. Pickart and R. Nathans, J. Appl. Phys. **33**, 1336 (1962).
[16] Produced by Metals Research Ltd. Melbourne, Royston Herts, England.

periments were disks 10 mm in diameter and 0.3–0.6 mm thick. Their mosaic-spread parameters η, defined according to Bacon,[17] were found to range from 0.3° to 0.6°. The sample used for the magnetization measurements was a cylinder 2 cm long.

B. Magnetization Measurements

The determination of the bulk magnetization was performed by the ballistic method using a nickel sample of identical shape for calibration purpose. Its value for $MnPt_3$ at liquid-nitrogen temperature was found to be $n=(4.04\pm0.08)\ \mu_B$ per unit cell, in satisfactory agreement with the value $n=(4.12\pm0.08)\ \mu_B$ given by Pickart and Nathans,[15] and also with the value $n=3.9\ \mu_B$ which can be estimated from measurements published by Auwärter and Kussman.[18]

C. Polarized Neutron Technique

This technique has been described in detail by Nathans *et al.*[19] The ratio γ of the magnetic to the nuclear structure factors is obtained directly from the ratio of the diffracted intensities of neutrons polarized parallel and antiparallel to the direction of the magnetic field applied to the sample. The magnetic field was 7 kOe and the sample was kept at liquid-nitrogen temperature.

The main sources of errors are depolarization of the incident and diffracted beam in the sample and the cryostat walls, and multiple scattering, extinction, and contamination of half-wavelength neutrons in the monochromatic beam.

Depolarization and multiple scattering were experimentally checked and accounted for using standard procedures.[7,8]

The presence of secondary extinction was checked by measuring the γ values as a function of both the length of the neutron optical path in the samples and the neutron wavelength $0.80\ \text{Å}\leq\lambda\leq1.20\ \text{Å}$. The γ values were found to be affected by extinction by less than 3% and were corrected by extrapolation to zero optical path of the neutron beam and zero neutron wavelength. The correctness of this procedure was tested by directly measuring the amount of extinction present in some reflections. The measurement was performed by observing the intensity variation of the beams diffracted and transmitted by the crystal when rocked through a Bragg position. The beam size was kept smaller than the crystal, and the counter accepted all diffracted or transmitted beams. The peak in the diffracted intensity and the dip in the transmitted intensity were found to be equal, point to point, within statistical errors. The fractional decrease of the transmitted beam in the case of symmetric transmission is a direct measurement of the amount of extinction.

As far as the higher-order contaminations were concerned, only $\frac{1}{2}\lambda$ was found to be appreciable in the λ range used by us. Corrections are larger for superlattice lines. A computer program was used to correct by an iterative procedure the γ values using the measured $\frac{1}{2}\lambda$ contamination. A maximum correction to superlattice lines of 1.5% was applied at 0.8 Å, and 3% at 1.2 Å.

III. UNPAIRED ELECTRON DENSITY

A. Magnetic Structure Factors

Measurements were performed out to $(\sin\theta)/\lambda=0.85\ \text{Å}^{-1}$, including all of the first 51 independent Bragg reflections. The results are shown in Fig. 1 and Table I.

The magnetic structure factors were calculated from the measured γ values; the values of the nuclear scattering lengths were taken from the literature[17]: $b_{Mn}=-0.36\times10^{-12}$ cm and $b_{Pt}=0.95\times10^{-12}$ cm. Errors quoted in Table I are either the standard deviations of repeated measurements or the uncertainties arising from the corrections discussed in Sec. II C; always the largest of the two has been given. There does not

TABLE I. Experimental magnetic structure factors in units of Bohr magnetons.

Fundamental reflections			Superlattice reflections		
	$(\sin\theta)/\lambda$	F_M		$(\sin\theta)/\lambda$	F_M
(hkl)	(Å^{-1})	(μ_B)	(hkl)	(Å^{-1})	(μ_B)
000	0	4.04 ±0.08	100	0.128	2.743±0.012
111	0.222	2.306±0.023	110	0.181	2.318±0.010
200	0.257	1.996±0.016	210	0.287	1.505±0.011
220	0.363	1.028±0.020	211	0.314	1.252±0.008
311	0.425	0.648±0.017	300	0.385	0.879±0.017
222	0.444	0.581±0.021	221	0.385	0.862±0.015
400	0.513	0.358±0.019	310	0.406	0.757±0.016
331	0.559	0.245±0.018	320	0.462	0.564±0.017
420	0.574	0.216±0.022	321	0.480	0.518±0.016
422	0.628	0.117±0.020	410	0.529	0.378±0.020
511	0.666	0.125±0.030	322	0.529	0.311±0.021
333	0.666	0.088±0.022	411	0.544	0.358±0.021
440	0.725	0.039±0.020	330	0.544	0.282±0.012
531	0.759	−0.01 ±0.03	421	0.588	0.28 ±0.04
600	0.769	0.02 ±0.03	332	0.602	0.13 ±0.03
442	0.769	−0.02 ±0.04	500	0.641	0.07 ±0.02
620	0.811	0.03 ±0.04	430	0.641	0.16 ±0.03
533	0.841	0.04 ±0.04	510	0.654	0.16 ±0.03
622	0.851	0.03 ±0.05	431	0.654	0.15 ±0.02
			520	0.691	0.07 ±0.03
			432	0.691	0.09 ±0.02
			521	0.702	0.06 ±0.03
			522	0.737	0.12 ±0.03
			441	0.737	0.00 ±0.03
			530	0.748	0.01 ±0.02
			433	0.748	−0.01 ±0.03
			610	0.780	−0.01 ±0.03
			611	0.791	−0.01 ±0.05
			532	0.791	0.06 ±0.03
			621	0.821	0.03 ±0.03
			540	0.821	−0.04 ±0.03
			443	0.821	−0.01 ±0.04
			541	0.831	0.01 ±0.04

[17] G. E. Bacon, *Neutron Diffraction* (Oxford University Press, New York, 1962), pp. 31, 66.
[18] M. Auwärter and A. Kussman, Ann. Physik **7**, 169 (1950).
[19] R. Nathans, C. G. Shull, G. Shirane, and A. F. Andresen, J. Phys. Chem. Solids **10**, 138 (1959).

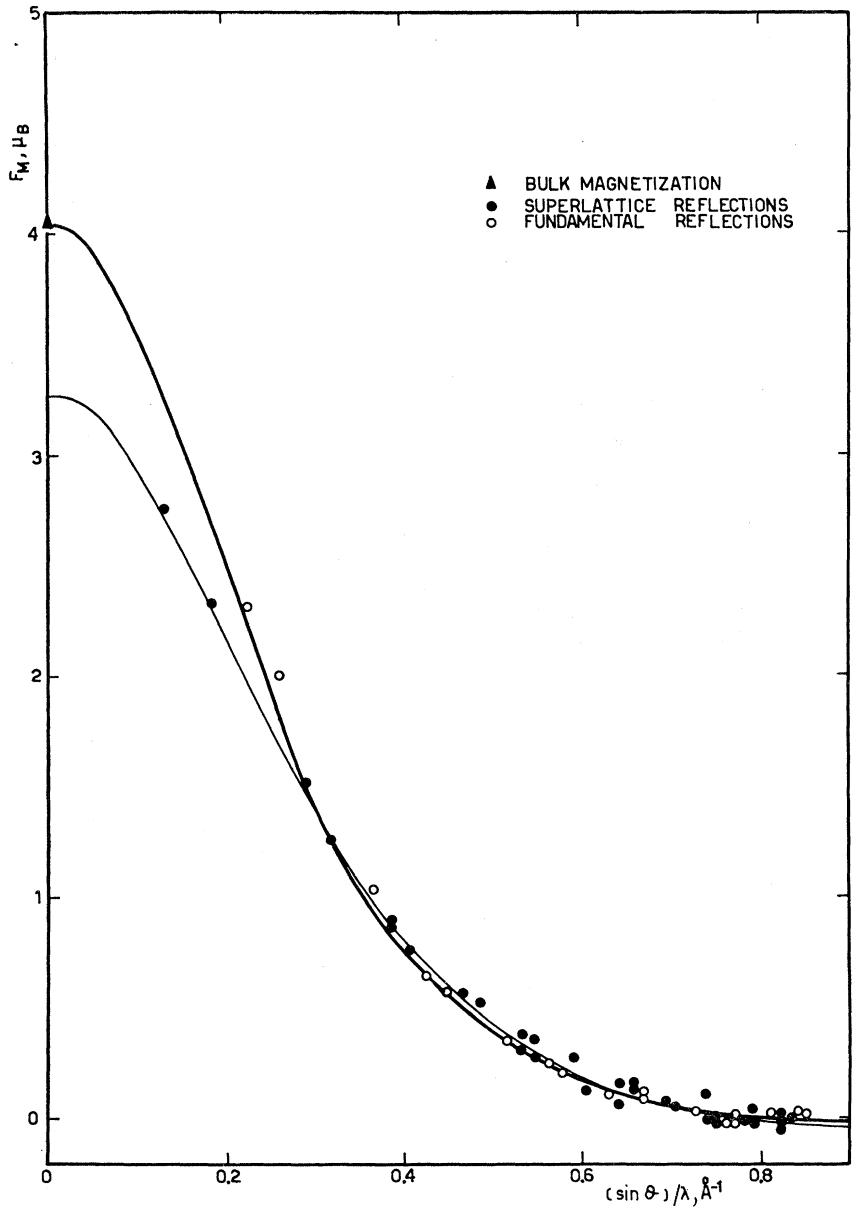

FIG. 1. Experimental magnetic structure factors in units of Bohr magnetons per unit cell. The two curves were obtained by assigning $\pm 3.64\ \mu_B$ to the Mn atom (+, or − sign for Mn atoms in Mn or Pt sites, respectively) and $0.26\ \mu_B$ to the Pt atom, and by using the following theoretical form factors: for Mn the free-atom form factor calculated by Freeman and Watson (Ref. 22) for the $3d$ shell in the configuration $3d^5 4s^2$, for Pt the free-atom form factor calculated by Cromer and Waber (Ref. 24) for the $5d_{5/2}$ shell in the double-ionized configuration. The dark line shows the fundamental reflections. The light line shows the superlattice reflections.

seem to be any reliable procedure of correcting the magnetic structure factors for thermal vibrations. In fact, since in an ordered structure the sublattices vibrate with temperature in different ways,[20] it is expected that the Debye-Waller factors are different for the Pt and Mn sites; therefore, the temperature factors do not simply cancel out in the measured ratio γ of magnetic to nuclear structure factors, as is the case for pure elements (under the hypothesis that magnetic electrons and nuclei are vibrating as a whole). However, a rough estimate of the effect of the temperature factor was attempted under the extreme hypothesis that both the platinum and manganese sublattices are vibrating as in the pure Pt and Mn metals. It was found that the maximum effect [obtained at $(\sin\theta)/\lambda = 0.85\ \text{Å}^{-1}$] was -1% for the superlattice lines and $+0.5\%$ for the fundamental ones. As this correction was so small and doubtful, it was neglected thereafter.

B. Magnetic Moments and Form Factors

It can be seen in Fig. 1 that the superlattice and fundamental structure factors lie on different curves. This indicates the presence of a magnetic moment on the platinum site. It is known[2] that the platinum form factor falls off much more rapidly with $(\sin\theta)/\lambda$ than the form factor of Mn, and has its first zero at $(\sin\theta)/\lambda$

[20] I. Waller and R. W. James, Proc. Roy. Soc. (London) **A117**, 214 (1927).

$\simeq 0.4$ Å^{-1}. In fact, it is observed that the superlattice structure factors become slightly larger than the fundamental ones at $(\sin\theta)/\lambda > 0.4$ Å^{-1}. This fact indicates that the magnetic moment one observes on the platinum sites is to be ascribed substantially to $5d$ electrons.

To obtain the distribution of the magnetic moment there are two possible approaches: We can either fit the observed magnetic structure factors with theoretical form factors keeping the magnetic moments as free parameters, or directly integrate the magnetic moments from the Fourier inversion of the data. The first method introduces the hypothesis that the available theoretical form factors, calculated for free atoms, can be employed for atoms in metals; the other method can be applied only if there is no appreciable overlapping of the atoms. We decided to use the last approach, since it does not introduce any *a priori* hypothesis on form factors.

As is well known, the magnetic structure factors can be considered the coefficients of a Fourier expansion of the magnetization density $\rho(x,y,z)$. Therefore, by Fourier inversion of the data, one obtains $\rho(x,y,z)$ from the equation

$$\rho(x,y,z)=\frac{1}{V}\sum_{h=-\infty}^{\infty}\sum_{k=-\infty}^{\infty}\sum_{l=-\infty}^{\infty}F_{hkl}e^{2\pi i(hx+ky+lz)}, \quad (1)$$

where V is the unit-cell volume, h, k, and l are the Miller indices of a reflection, and F_{hkl} is its measured structure factor. Although the sums extend to infinity, in all practical cases they are limited to finite values of the Miller indices, and therefore termination errors are expected to be present. A means of reducing these errors below a given value was suggested by Shull and coworkers[6–8] and consists in calculating the averaged value of the density over a selected volume rather than the point density of Eq. (1). In this case, we have

$$\bar{\rho}(x,y,z)=\frac{1}{V}\sum_{h=-\infty}^{\infty}\sum_{k=-\infty}^{\infty}\sum_{l=-\infty}^{\infty}F_{hkl}\frac{\sin 2\pi h\delta}{2\pi h\delta}\times\frac{\sin 2\pi k\delta}{2\pi k\delta}\frac{\sin 2\pi l\delta}{2\pi l\delta}e^{2\pi i(hx+ky+lz)}, \quad (2)$$

where 2δ is the edge of the cubic volume, centered at the point (x,y,z), over which the average is taken. Each structure factor is now multiplied by a factor, which is smaller the higher the order of the reflection; thus, the convergence of the series, Eq. (2), is faster than that of Eq. (1), and by choosing a suitable δ one can obtain a value of $\bar{\rho}$ which is not appreciably affected by termination errors. The proper value of δ is set by the maximum value of $(\sin\theta)/\lambda$. In our case, we found that $\frac{1}{10}$ of the lattice parameter was adequate in order to obtain values of $\bar{\rho}$, which were not appreciably affected by extending the range of $(\sin\theta)/\lambda$ from 0.75 to 0.85 Å^{-1}. Some representative results of this Fourier inversion are shown in Fig. 2. Contour lines are affected by an error of the order of 0.02 μ_B/Å^3 estimated according to the procedure suggested by Lipson and Cochran.[21] From the comparison of the nonaveraged magnetization distribution obtained with $(\sin\theta)/\lambda \leq 0.75$ and ≤ 0.85 Å^{-1}, respectively, it can be seen that some general features are already established at $(\sin\theta)/\lambda = 0.75$ Å^{-1}, e.g., the asphericity of the Pt atom and the almost spherical character of Mn. Some details like the positions of the low-level contour lines and some of the negative-magnetization areas appear to change with different terminations. The averaged distributions shown in Fig. 2 do not show most of these details, which consequently are presumed to be due to the termination errors. However, some of the asphericities are smoothed, but this could be expected from an averaging procedure of this kind, we believe that they are real because of their relative insensitivity to different terminations.

One can observe that the magnetization at the platinum sites is clearly distinguishable from that at the manganese site, although they overlap slightly, a line could be traced through the middle of the shallow region of minimum magnetization density, lying between the two atomic sites. This line was assumed to represent the boundary between Mn and Pt sites. A set of sections of $\bar{\rho}(x,y,z)$ was calculated for $\delta=\frac{1}{10}$ of the cell edge, including all reflections out to $(\sin\theta)/\lambda = 0.85$ Å^{-1}. Summations of $\bar{\rho}(x,y,z)$ at all of the points lying on each side of the boundary line were carried out and gave the following magnetic moments: 3.46 μ_B for Mn site and 0.19 μ_B for Pt site.

It is a difficult task to calculate the extent to which the statistical errors on the contour lines affect the magnetic moment; however, they should partially compensate. The use, in this instance, of the averaged magnetization density rather than the point density was found convenient in order to reduce the spurious details due to the termination.

It should be noted that because of the imperfect long-range order, the values of the magnetic moments at Mn and Pt sites do not coincide with the magnetic moments associated with Mn and Pt atoms. In order to calculate them some assumptions are then necessary.

If we assume that all the moments of Pt and Mn stay constant in value and orientation, independently of the site, we obtain

$$\mu_{\mathrm{Mn}}=(3.68\pm0.08)\,\mu_B \quad \text{and} \quad \mu_{\mathrm{Pt}}=(0.12\pm0.03)\,\mu_B.$$

This set of values would imply that at the center of the Pt atom a very deep negative-magnetization region should be present. In fact, we must account for the experimental negative density of -0.025 μ_B/Å^3 found at the center of the Pt site (Fig. 2) as resulting from the superimposition of 1.8% Mn atoms and 98.2% Pt

[21] H. Lipson and W. Cochran, *The Determination of Crystal Structures* (G. Bell and Sons, London, 1957), p. 288.

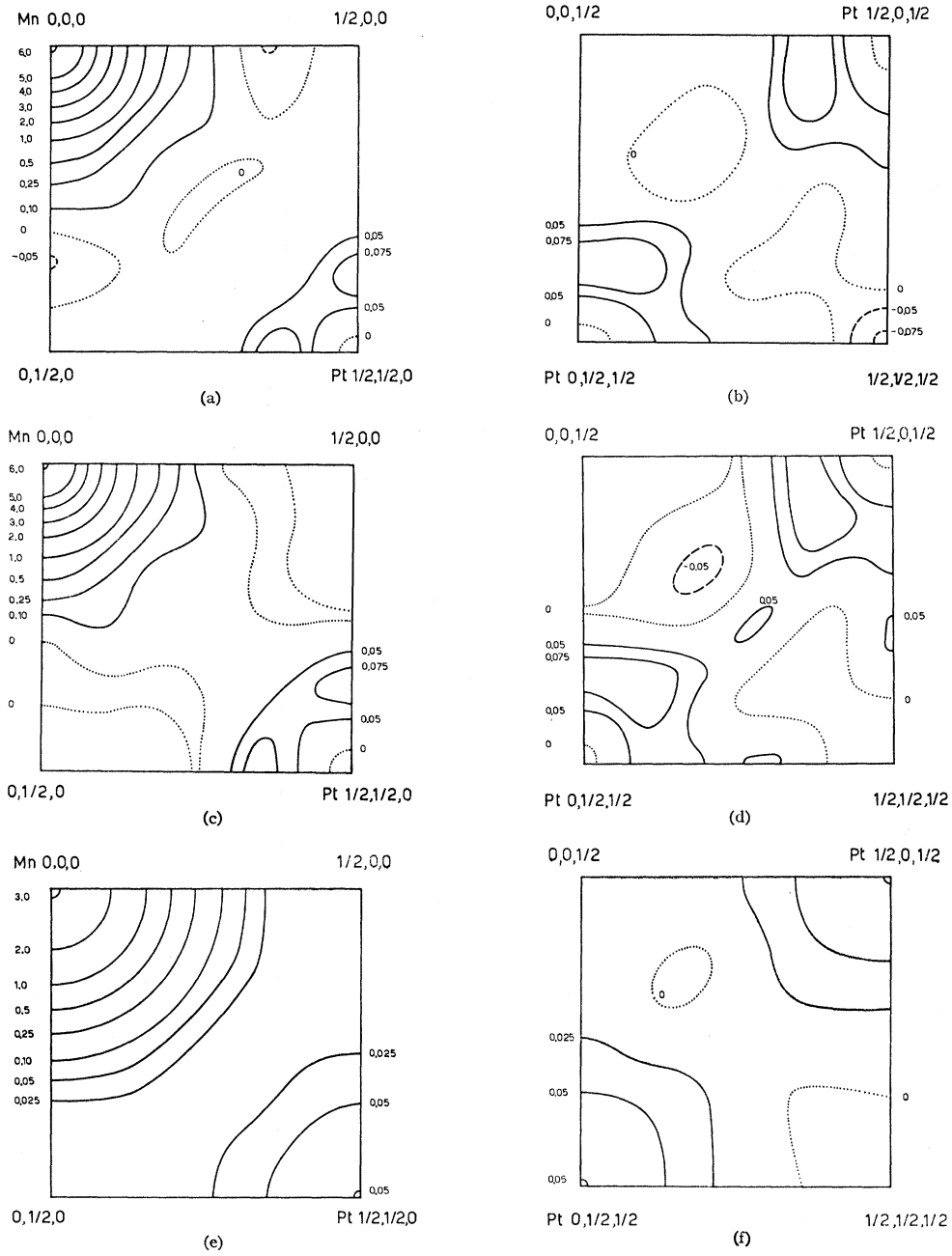

FIG. 2. Sections of the magnetic electron distribution obtained by Fourier inversion of the data. Contours are expressed in $\mu_B/\text{Å}^3$. (a) $\frac{1}{4}$ of the section on a basal plane including all reflections out to $(\sin\theta)/\lambda=0.75$ Å^{-1}, (b) $\frac{1}{4}$ of the section parallel to a basal plane, through the center of the cell, including all reflections out to $(\sin\theta)/\lambda=0.75$ Å^{-1}, (c) same as (a), including all reflections out to $(\sin\theta)/\lambda=0.85$ Å^{-1}, (d) same as (b), including all reflections out to $(\sin\theta)/\lambda=0.85$ Å^{-1}, (e) same as (c), integrated over a volume $8\delta^3$ as described in the text, and (f) same as (d), integrated over a volume $8\delta^3$ as described in the text. In sections (a) to (d) the zero contour lines enclose regions of negative-magnetic density which reach the level 0.025 $-\mu_B/\text{Å}^3$ at the center of the Pt site.

atoms (these atomic populations correspond to the measured long-range order parameter $S=0.92$).

If the moment is taken to be the same for Mn atoms on both Mn and Pt sites, then a negative-magnetization density of -0.15 $\mu_B/\text{Å}^3$ at the center of Pt atoms would be required. On the basis of both neutron experiments in ferromagnetic elements,[6,8] and theoretical calculations, the presence of such a strong negative-magnetization density at the center of a ferromagnetic atom seems to be very unlikely.

On the other hand, if we drop the hypothesis that the Mn moments are independent of the site, one sees

immediately that our experimental data can be explained by assuming an antiparallel orientation of the moments of Mn atoms located at Pt sites. It seems reasonable that in $MnPt_3$ as well, the magnetization density at the center of Pt atoms would be of the same order of magnitude as the one measured in the fully ordered $CoPt_3$, i.e., 0.05 $\mu_B/Å^3$.[2] The negative density at the center of Pt sites would then be accounted for by assuming that the 1.8% Mn atoms present, because of the incomplete order, would carry a moment of about the same magnitude but of opposite orientation of the ones at Mn sites.

Such an hypothesis is consistent with the fact that for Mn-Mn pairs an antiferromagnetic interaction is usually found, and indeed any Mn atom on Pt sites has four Mn nearest neighbors. Experimental support for our point of view is provided by other measurements in the Mn-Pt system which indicate a sharp maximum in the bulk magnetization[18] at $Mn_{0.25}Pt_{0.75}$,[18] and antiferromagnetic ordering[14] at $Mn_{0.50}Pt_{0.50}$ composition. The values of Mn and Pt moments turn out to be $\mu_{Mn}=(3.64\pm0.08)\ \mu_B$ and $\mu_{Pt}=(0.26\pm0.03)\ \mu_B$, if Mn atoms located at Pt sites are assumed to be antiferromagnetic, while Pt atoms at Mn sites are assumed to keep both magnitude and orientation of their magnetic moments. It should be considered also that any orientation change of the moment on Pt atoms with site would, in any case, affect the given results by no more than 1%.

By using the values of magnetic moments obtained above, one can now calculate the individual form factors f_{Pt} and f_{Mn}. First, we considered only the spherical part of the form factors by fitting a smooth curve to the experimental points for each kind of reflections. It was then possible to solve the two equations for f_{Mn} and f_{Pt}. The experimental form factor of Mn was found to be very close to the one calculated by Freeman and Watson[22] using a Hartree-Fock approach for the electron configuration $3d^54s^2$ (Fig. 3); the Mn form factor obtained for the $3d^7$ electron configuration by Watson and Freeman[23] was definitely inconsistent with the result of the present experiment. The contribution of the unknown orbital moment has been neglected in our treatment. However, one must consider that all previous measurements on d transition metals indicate that orbital contribution affect the neutron results very slightly.[6–8] Similarly, the Pt form factor was compared

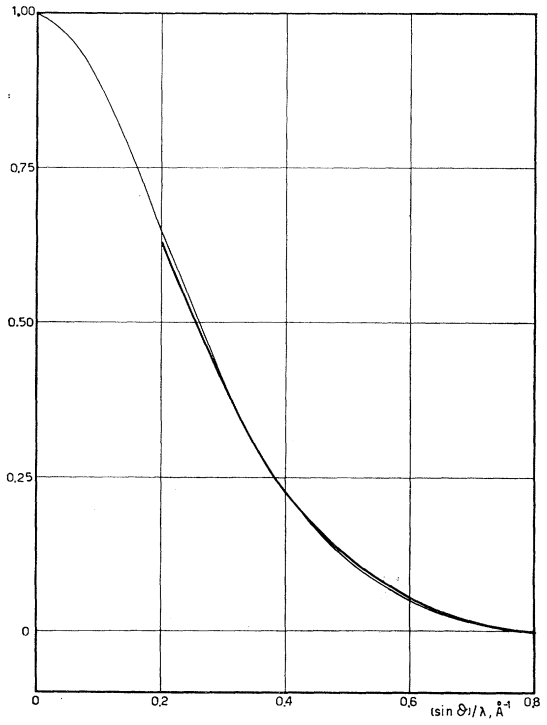

FIG. 3. Comparison of experimental and theoretical spherical form factors of Mn. The thin curve has been calculated by Freeman and Watson (Ref. 22). The dark line has been obtained from the smoothed magnetic structure factors. The uncertainty in the form factor arising from experimental errors is estimated to range from 0.014 at $(\sin\theta)/\lambda=0.2$ Å^{-1} to 0.006 at $(\sin\theta)/\lambda=0.8$ Å^{-1}.

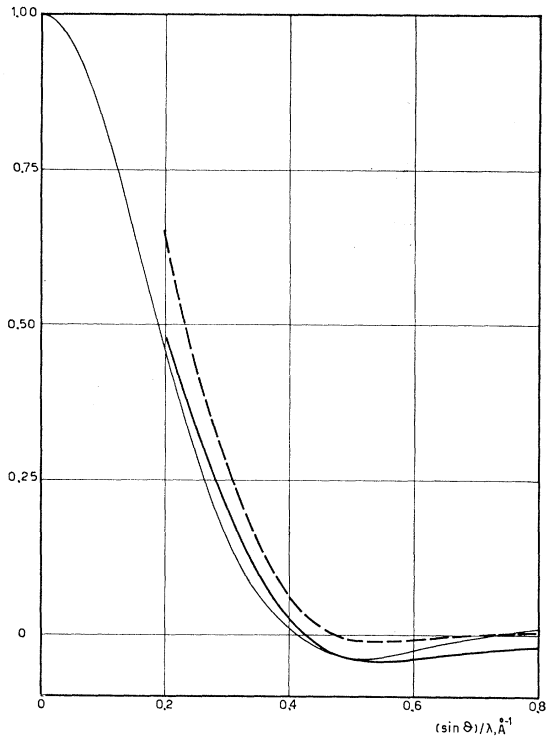

FIG. 4. Comparison of experimental and theoretical spherical form factors of Pt. The light line has been calculated by Cromer and Waber (Ref. 24). The dashed curve has been obtained from the smoothed magnetic structure factors in $MnPt_3$ alloy. The dark line is the experimental Pt form factor in $CoPt_3$ alloy (Ref. 2). The uncertainty in the form factor arising from experimental errors is estimated to range from 0.11 at $(\sin\theta)/\lambda=0.2$ Å^{-1} to 0.04 at $(\sin\theta)/\lambda=0.8$ Å^{-1}.

[22] A. J. Freeman and R. E. Watson, Acta Cryst. 14, 231 (1961).
[23] R. E. Watson and A. J. Freeman, Acta Cryst. 14, 27 (1961).

with the previous determination obtained for $CoPt_3$ alloy,[2] and with the theoretical one obtained by Cromer and Waber[24] with a relativistic Hartree-Fock-Slater calculation; the experimental form factor was found to be slightly more expanded (Fig. 4).

Some areas of negative magnetization are observed in the Fourier inversion of the data beside the ones at the center of Pt sites. They are at the center of the cell and around the point at approximately $(\frac{1}{4},\frac{1}{4},\frac{1}{3})$ and its equivalents. They do not seem to depend on series termination errors and do not appear to be part of a constant "sea" of negative polarized conduction electrons, since this would give a distribution of magnetic moments definitely inconsistent with the calculated form factors. We are inclined to think that spin-polarization effects in the d band should be the correct explanation to these observed negative polarization areas. In this case, most of the magnetic moment should be ascribed to the electrons at the top of the d band, which are known to have wave functions very similar to the free-atom ones. This would explain why free-atom theoretical form factors provide a good fit to the experimental data, as shown in Fig. 1.

C. Asphericities

Figure 1 shows that reflections at the same $(\sin\theta)/\lambda$ have different structure factors. This is a consequence of the anisotropy of magnetization distribution. It can be seen in Fig. 2 that the asphericity of the Pt atoms is very pronounced and is not strongly dependent on series termination. This appears to be a common characteristic of the $5d$ and $4d$ metals so far investigated, which we have observed in $CoPt_3$ [2] and FeRh.[4] The Pt atoms appear to have equal lobes along the two crystallographic axis on the basal plane, and a different distribution along the axis pointing towards the center of the cell. This is due to the tetragonal symmetry of the Pt environment. A tetragonal crystalline field splits the fivefold degenerate electronic d level of an atom into four sublevels, while a cubic field splits it into two sublevels. In a field with a tetragonal axis z, the cubic E_g level is split into two singlets A_1 and B_2 with rotational properties $3z^2-r^2$ and x^2-y^2, respectively, while the T_{2g} is split[25] into a singlet $B_1(xy)$ and a doublet $E(xz,yz)$ (Fig. 5).

The Mn atom, which is in a cubic environment, appears to be much more spherical than Pt. This is in agreement with the fact that Mn should have an almost closed shell of d electrons in the metallic state, i.e., close to the $3d^5$ configuration of the free atom. In fact, the $3d^5$ theoretical form factor is in good agreement with our results. The small asphericity present was found to be due to a population of the E_g level of

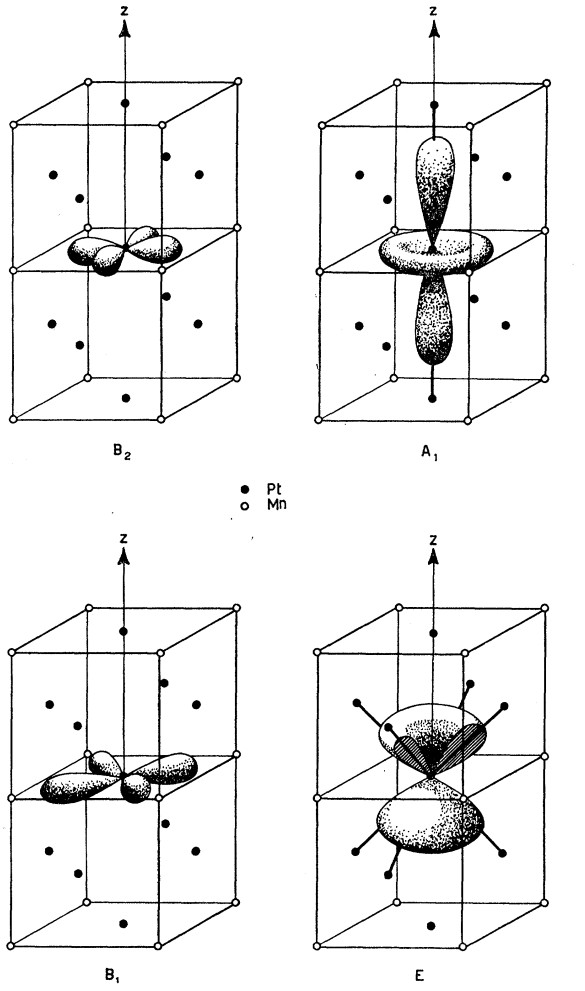

FIG. 5. Sketch of the angular distribution of the d-sublevel charge density in a tetragonal field.

0.43 ± 0.02 (0.40 is the value for spherical distribution), following the treatment of Weiss and Freeman[26]; the aspherical part of the form factor $\langle j_4\rangle$ used in this evaluation was the one calculated by Watson and Freeman[23] for Mn in the $3d$ configuration.[7] The aspherical form factor $\langle j_4\rangle$ of Pt, unavailable in the literature, was obtained by double Fourier inversion from the experimental spherical form factor of Pt in $CoPt_3$ alloy.[2]

We found the following populations for Pt sublevels: 0.15 in A_1, 0.27 in B_2, 0 in B_1, and 0.58 in E; the uncertainty is estimated to be 0.05. This means that $5d$ electrons in Pt are concentrated toward both nearest neighbors and next-nearest neighbors. These populations were evaluated by comparing the magnetization-density maps obtained by Fourier inversion of the measured structure factors with the ones calculated for

[24] D. T. Cromer and J. T. Waber, Los Alamos Scientific Report No. LA-3056, 1964 (unpublished).

[25] M. Hamermesh, *Group Theory and Its Application to Physical Problems* (Pergamon Press, London, 1962), p. 344.

[26] R. J. Weiss and A. J. Freeman, J. Phys. Chem. Solids **10**, 147 (1959).

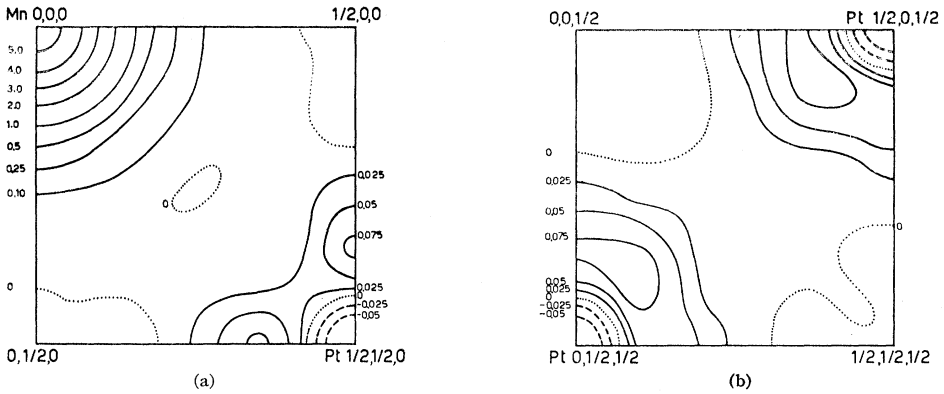

FIG. 6. Fourier inversion of the structure factors calculated by using the theoretical form factors of Mn (Refs. 22 and 23) and the experimental form factor of Pt (Ref. 2), with the distribution of magnetic moments and sublevel population as found in this work. (a) $\frac{1}{4}$ of the section on a basal plane, including all calculated reflections out to $(\sin\theta)/\lambda = 0.85$ Å^{-1}, and (b) $\frac{1}{4}$ of the section parallel to a basal plane, through the center of the cell, including all reflections out to $(\sin\theta)/\lambda = 0.85$ Å^{-1}.

several sets of sublevel populations. As a further check, a least-squares fit of calculated and experimental structure-factor differences was performed for all measured pairs of reflections. In this way, the contribution of the spherical part of the form factor was canceled out. The sections calculated with the given set of populations are shown in Fig. 6.

IV. CONCLUSIONS

The magnetic moments associated with Mn and Pt in this alloy are very close to those found in other alloys containing Mn or Pt, i.e., approximately $\frac{1}{4}\ \mu_B$ for Pt and $3\frac{3}{4}\ \mu_B$ for Mn, which is an indication of a prevalent localized character of the magnetic moment. This view is supported by the Fourier inversion of the experimental data and by the fact that the form factors substantially agree with those calculated for free atoms.

A comparison with previous results in Fe-Rh and $CoPt_3$ seems to indicate a trend toward asphericity of $4d$ and $5d$ electrons.

ACKNOWLEDGMENTS

We wish to thank Dr. F. Leoni and Dr. C. Natoli, who have derived an expression for the aspherical contribution to form factors for atoms in tetragonal environments. We are also indebted to Dr. M. Diana and Dr. G. Mazzone, who have determined the long-range order parameter by means of x-ray diffraction. We thank all the staff of the RC-1 reactor for their cooperation.